Periodic, quasiperiodic, and chaotic localized solutions of a driven, damped nonlinear lattice

Dirk Hennig
Fachbereich Physik, Institut für Theoretische Physik Arnimallee 14, Freie Universität Berlin, 14195 Berlin, Germany
(Received 21 August 1998)

We study the solution behavior of a damped and parametrically driven nonlinear chain modeled by a discrete nonlinear Schrödinger equation. Special attention is paid to the impact of the damping and driving terms on the existence and stability of localized solutions. Dependent upon the strength of the driving force, we find rich lattice dynamics such as stationary solitonlike solutions and periodic and quasiperiodic breathers, respectively. The latter are characterized by regular motion on tori in phase space. For a critical driving amplitude the torus is destroyed in the course of time, leaving temporarily a chaotic breather on the lattice. We call this order-chaos transition a dynamical quasiperiodic route to chaos. Eventually the chaotic breather collapses to a stable localized multisite state. Finally, it is demonstrated that above a certain amplitude of the parametric driving force no localized states exist. [S1063-651X(99)04202-6]

PACS number(s): 05.45.Xt, 41.20.Jb, 63.20.Pw, 63.20.Ry

I. THE DAMPED, DRIVEN, NONLINEAR, DISCRETE SCHRÖDINGER EQUATION

The influence of dissipation on the excitation of coherent structures, especially solitons, in various physical model systems was studied in a series of papers over the past two decades [1–5]. Because of its important role in describing soliton dynamics in nonlinear media [6], special attention was paid to the nonlinear Schrödinger (NLS) equation modified by the inclusion of damping and driving terms [7,2]. Barashenkov *et al.* [2,8] studied the parametrically driven, damped NLS equation $i\Psi_t+\partial^2\Psi/\partial x^2+2|\Psi|^2\Psi=h\Psi^*\exp(i\Omega t)-i\delta\Psi$, where $\Psi(x,t)$ is a complex field amplitude. They found that stable localized solutions in the form of solitons are excitable only if the strength of the driving field h exceeds the damping constant δ, that is, $h>\delta$. In particular, in the absence of the driving field the damped NLS equation does not support soliton solutions for any $\delta>0$.

However, the application of the continuum NLS equation is justified only if the spatial extension of the nonlinear waves is much larger than typical inherent length scales of the system (e.g., the distance between adjacent fibers in arrays of coupled optical waveguides). Otherwise, the discrete structure of the system has to be taken into account and we must consider the discretized system rather than the continuum equation. Furthermore, whenever a numerical study of the nonlinear wave equation is demanded the issue of its discretization has to be addressed. One possible discretization of the parametrically driven, damped NLS equation is given by

$$i\frac{\partial\Psi_n(t)}{\partial t}+2|\Psi_n(t)|^2\Psi_n(t)+V[\Psi_{n+1}(t)+\Psi_{n-1}(t)-2\Psi_n(t)]=h\Psi_n^*(t)\exp(i\Omega t)-i\delta\Psi_n(t). \quad (1)$$

The real parameters $\delta\geqslant 0$ and $h\geqslant 0$ determine the strength of the damping and driving force, respectively. We introduced the real parameter V regulating the strength of the coupling between the lattice oscillators. In the conservative, undriven limit of $\delta=0$ and $h=0$ Eq. (1) reduces to the standard DNLS system, which finds application in numerous physical fields [9]. However, the standard DNLS equation is nonintegrable [10,11] and therefore does not exhibit exact soliton solutions. Nevertheless, as shown in [12], the excitation of stable localized states provided by stationary solitonlike solutions is possible. Furthermore, the standard DNLS equation represents a Hamiltonian lattice for which the existence of breather solutions, that is, spatially localized and time-oscillating solutions, is well established [13,14]. MacKay and Aubry have proved that for time-reversible Hamiltonian networks of weakly coupled oscillators the trivial localized solutions of the no-coupling limit are continued for small coupling strengths as time-periodic and exponentially localized states provided certain anharmonicity and nonresonance conditions are fulfilled [13]. Using the continuation method without time-reversal symmetry, Sepulchere and MacKay have extended the result to more general oscillator networks, including also dissipative systems [15]. The concept of the continuation of localized solutions starting from the anticoupling limit has been exploited by Johansson and Aubry to construct quasiperiodic breathers of the standard DNLS equation oscillating with two incommensurate frequencies [16]. In Ref. [17] the quasiperiodic breathers of the Ablowitz-Ladik discretization [18,19] of the NLS equation have been derived with the help of the inverse scattering transformation. Konotop *et al.* [20] and Cai *et al.* [21] proved integrability of the dynamics of the Ablowitz-Ladik system in a time-varying, spatially uniform electric field along the chain direction, which is of the form $V_n=\mathcal{E}(t)n$. However, less work has been done with respect to the mutual impact of dissipation and driving forces on breather solutions [22].

The scope of the present study is to demonstrate that the driven, damped DNLS lattice exhibits rich dynamical localization effects. Various types of localized lattice states arise, namely, periodic and quasiperiodic breathers, respectively, and a form of localized spatiotemporal chaos, which we call a chaotic breather. The formation of the chaotic breather re-

sults from a dynamical bifurcation for which quasiperiodic motion persists as a regular transient evolution at the end of which it becomes destabilized and the associated torus is destroyed. The chaotic breather sustains temporarily on the lattice and collapses finally to a stable localized multisite pattern.

In Sec. II we investigate the stationary system with emphasis on the existence of localized solitonlike states. The stationary system can be formulated in terms of a four-dimensional volume-preserving map. We identify parameter constellations for which the origin represents a hyperbolic equilibrium. The attributed homoclinic orbit is exploited to construct a solitonlike state on the damped, driven lattice. Linear stability of the stationary localized solution is discussed with the help of Floquet analysis. Section III deals with the dynamical features of the damped, driven DNLS lattice. First, we discuss the case of vanishing lattice couplings $V=0$ for which a set of uncoupled driven, damped oscillators is obtained. The dynamics of a single oscillator is then investigated. In particular we search for parameter values for which, in addition to the stable zero point, a second (nonzero) attractor exists on the Poincaré map of the oscillator providing a periodic solution. In order to construct a localized lattice state only one oscillator is excited initially in the periodic regime and the remaining ones are held at the zero fixed point (the single oscillator lattice excitation). This yields a trivial localized lattice solution, that is, a one-site breather. When the oscillators become coupled ($V>0$) this simple localized state experiences a continuation as a static breather up to some driver amplitudes. Interestingly, when the amplitude of the driving force is further enlarged the static breathers changes into quasiperiodic breathers as the result of a Hopf bifurcation, which is well illustrated on a two-dimensional return map assigned to a local oscillator. At a critical coupling strength we observe that the quasiperiodic breather becomes dynamically unstable, developing spatiotemporal chaos, which, remarkably, stays localized at a few lattice sites. Eventually, after the chaotic interlude is over a stable localized multisite state is reached. Finally, we demonstrate that above a certain amplitude of the driving the breather becomes dynamically unstable and is extinguished by collapsing to vanishing lattice amplitudes.

II. STATIONARY LOCALIZED SOLUTIONS

We study stationary solutions of the system (1) that are obtained from the ansatz

$$\Psi_n(t)=\phi_n e^{i\omega t}=(x_n+iy_n)e^{i\omega t}, \tag{2}$$

with $\phi_n\in C$ (real x_n,y_n) and a rotation frequency ω. Substituting Eq. (2) into Eq. (1), we obtain

$$\begin{aligned}&\omega\phi_n-2|\phi_n|^2\phi_n-V(\phi_{n+1}+\phi_{n-1}-2\phi_n)\\&\quad=i\delta\phi_n-h\phi_n^*\exp[i(\Omega-2\omega)t],\end{aligned} \tag{3}$$

from which we infer that stationary solutions are possible when the driving and rotation frequencies fulfill the condition

$$\Omega-2\omega=2k\pi,\quad k=0,\pm1,\pm2,\ldots. \tag{4}$$

Decomposing into real and imaginary part, we obtain

$$\omega x_n-2(x_n^2+y_n^2)x_n-V(x_{n+1}+x_{n-1}-2x_n)=-\delta y_n-hx_n \tag{5}$$

$$\omega y_n-2(x_n^2+y_n^2)y_n-V(y_{n+1}+y_{n-1}-2y_n)=\delta x_n+hy_n. \tag{6}$$

Setting $u_n=x_{n-1}$ and $v_n=y_{n-1}$, we express this difference system as a four-dimensional map $R^4\to R^4$ determined by

$$\mathcal{M}:\begin{cases}x_{n+1}=\dfrac{1}{V}[\tilde{\omega}x_n-2(x_n^2+y_n^2)x_n+hx_n+\delta y_n]-u_n,\\ y_{n+1}=\dfrac{1}{V}[\tilde{\omega}y_n-2(x_n^2+y_n^2)y_n-hy_n-\delta x_n]-v_n,\\ u_{n+1}=x_n,\\ v_{n+1}=y_n,\end{cases} \tag{7}$$

where $\tilde{\omega}=\omega+2V$ and we drop the tilde afterward. The map $\mathcal{M}$ is volume preserving because the Jacobian matrix $D\mathcal{M}$, which is given by

$$D\mathcal{M}=\begin{pmatrix}D_x & D_- & -1 & 0\\ D_+ & D_y & 0 & -1\\ 1 & 0 & 0 & 0\\ 0 & 1 & 0 & 0\end{pmatrix}, \tag{8}$$

with

$$D_x=\frac{1}{V}[\omega-6x_n^2-2y_n^2+h], \tag{9}$$

$$D_y=\frac{1}{V}[\omega-6y_n^2-2x_n^2-h], \tag{10}$$

$$D_\pm=-\frac{1}{V}[4x_ny_n\pm\delta], \tag{11}$$

fulfills the condition $\det D\mathcal{M}=1$.

Being interested in the excitation of localized states on the damped, driven lattice, we recall that such localized stationary solutions correspond to map orbits lying on the stable and unstable manifolds of hyperbolic equilibria. In particular a bright solitonlike solution is given by the homoclinic orbit associated with an unstable hyperbolic equilibrium point at the map origin.

Apparently, the origin $(x,y,u,v)=(0,0,0,0)$ represents an equilibrium point of the map $\mathcal{M}$. To investigate its spectral stability we need the characteristic polynomial $\det(D\mathcal{M}-\lambda I)=0$ associated with the tangent map at the origin, which reads

$$\lambda^4-A(\lambda^3+\lambda)+B\lambda^2+1=0, \tag{12}$$

with

$$A=\frac{2\omega}{V},\quad B=2+\frac{\omega^2-h^2}{V^2}-\frac{\delta^2}{V^2}. \tag{13}$$

Since the characteristic polynomial is reflexive it follows that complex eigenvalues occur generally in quadruplets $(\lambda,\lambda^{-1},\lambda^*,\lambda^{*-1})$. If $|\lambda|=1$ then they occur in complex conjugate pairs, while real eigenvalues come in pairs λ,λ^{-1} [23,24]. The eigenvalues are computed as

$$\lambda=\frac{1}{2}(\rho\pm\sqrt{|4-\rho^2|}), \tag{14}$$

with

$$\rho=\frac{1}{2}(A\pm\sqrt{A^2-4B+8}). \tag{15}$$

The origin (0,0,0,0) represents an unstable hyperbolic point if there exist two pairs of real eigenvalues $(\lambda_1,1/\lambda_1)$ and $(\lambda_2,1/\lambda_2)$ with $|\lambda|\neq 1$, which is the case if one of the following three constraints in parameter space is fulfilled:

$$A>4,\quad B>6,\quad 2(A-1)<B<\frac{A^2}{4}+2, \tag{16}$$

$$A<-4,\quad B>6,\quad -2(A+1)<B<\frac{A^2}{4}+2, \tag{17}$$

$$B<-2,\quad B<-2(A+1),\quad B<2(A-1). \tag{18}$$

In order to depict the homoclinic tangle of the invariant manifolds of the hyperbolic point we approximate the stable and unstable manifolds, respectively, in the vicinity of the hyperbolic point by the linear subspaces (straight lines in the direction of the eigenvectors to the eigenvalues with modulus unequal one) of the tangent map. After iteration of a few thousand points on them several times we obtain the homoclinic tangle. In Fig. 1 we plot the projections of the four-dimensional stable and unstable manifold of the hyperbolic equilibrium on the x-u plane, the y-v plane, and the x-y plane. One infers that there exist transversal intersections of the stable and unstable manifolds at isolated points forming a homoclinic orbit $\{\phi_n^{hom}\}$. It has been shown that homoclinic connections can be exploited to construct standing solitonlike solutions of lattice chains [12]. To this end we use the fact that homoclinic points approach the origin asymptotically along the stable (unstable) manifold for $n\to\infty$ $(-\infty)$, respectively. Therefore, the homoclinic orbit $\{\phi_n^{hom}\}$ is attributed to a localized state pinned by the lattice. Figure 2 shows such a stationary solitonlike excitation $|\Psi_n(t)|^2=|\phi_n^{hom}|^2$ of the damped, driven lattice. In this manner the damping term and the driving force conspire to support a coherent structure in the form of a bright solitonlike solution.

To investigate the linear stability of a time-periodic localized state $\Psi_n^{(0)}(t)=\phi_n^{hom}\exp(i\omega t)$ on the basis of the Floquet theory [25] we make the ansatz $\Psi_n(t)=\Psi_n^{(0)}(t)+\delta\Psi_n(t)$ including a small perturbation $\delta\Psi_n(t)$. The linear tangent equation for $\delta\Psi_n(t)$ reads

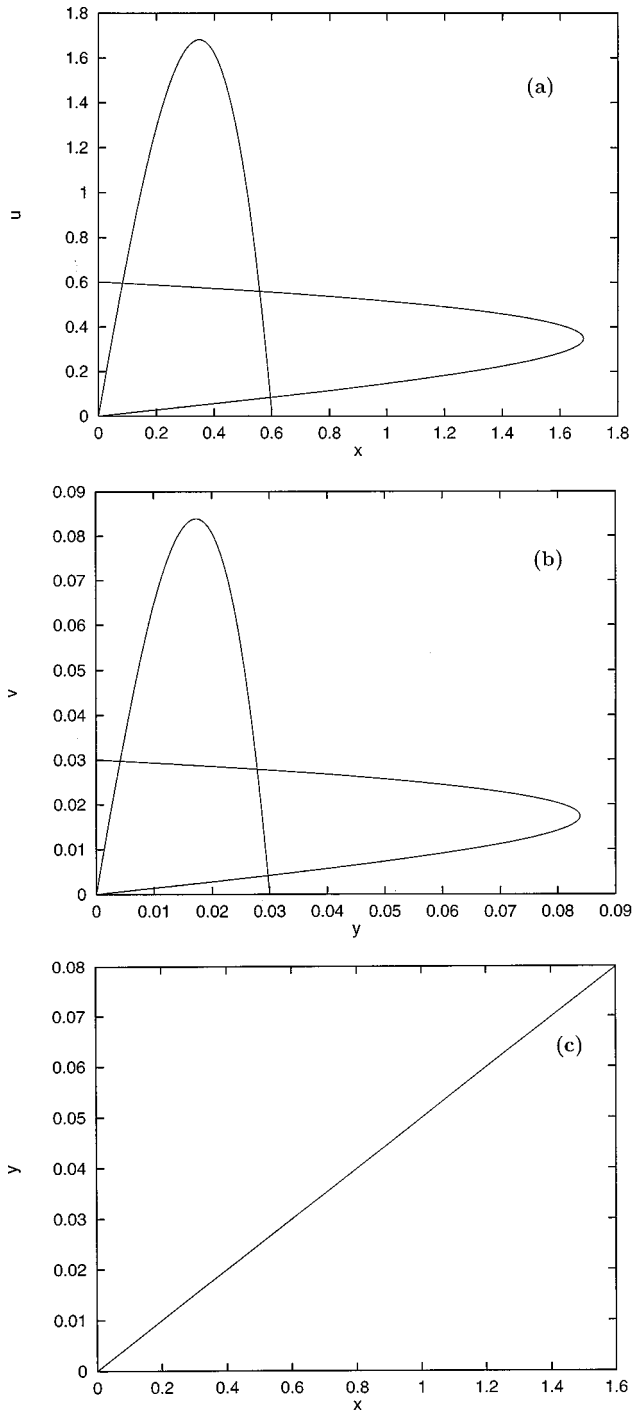

FIG. 1. Two-dimensional projections of the four-dimensional homoclinic tangle of the hyperbolic point (0,0,0,0). The parameters are $\delta=0.001$, $h=0.01$, $\omega=1.5$, and $V=0.1$. (a) The x-u plane. (b) The y-v plane. (c) The x-y plane.

$$\begin{aligned} i\delta\dot{\Psi}_n+2[2|\Psi_n^{(0)}|^2\delta\Psi_n+(\Psi_n^{(0)})^2\delta\Psi_n^*] \\ +V[\delta\Psi_{n+1}+\delta\Psi_{n-1}-2\delta\Psi_n] \\ =-i\delta\delta\Psi_n+h\delta\Psi_n^*\exp(i\Omega t). \end{aligned} \tag{19}$$

Decomposing into real and imaginary parts and using that $\delta\Psi_n=a_n+ib_n$, $\Psi_n^{(0)}(t)=\phi_n e^{-i\omega t}=(x_n+iy_n)e^{-i\omega t}$, and $\Omega-2\omega=2k\pi$, we obtain eventually

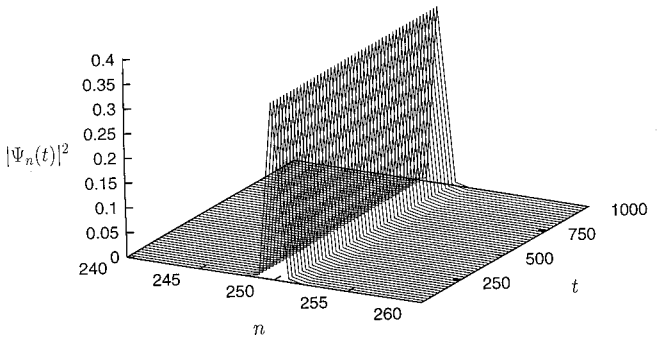

FIG. 2. Amplitude profile $|\Psi_n(t)|^2$ of the solitonlike solution derived from the homoclinic orbit of the stationary map. The parameters are the same as in Fig. 1.

$$\dot{a}_n = -2\{2(x_n^2+y_n^2)b_n+[2x_ny_n\sin(2\omega t) -(x_n^2-y_n^2)\cos(2\omega t)]b_n+[2x_ny_n\cos(2\omega t) +(x_n^2-y_n^2)\sin(2\omega t)]a_n\}-V[b_{n+1}+b_{n-1}-2b_n]-\delta a_n +h[a_n\sin(2\omega t)-b_n\cos(2\omega t)] \tag{20}$$

and

$$\dot{b}_n = 2\{2(x_n^2+y_n^2)a_n-[2x_ny_n\sin(2\omega t) -(x_n^2-y_n^2)\cos(2\omega t)]a_n+[2x_ny_n\cos(2\omega t) +(x_n^2-y_n^2)\sin(2\omega t)]b_n\}+V[a_{n+1}+a_{n-1}-2a_n] -\delta b_n-h[a_n\cos(2\omega t)+b_n\sin(2\omega t)]. \tag{21}$$

Integrating the tangent equations (20) and (21) over one period $T=2\pi/\omega$ yields a linear map

$$\begin{pmatrix} a_n(T) \\ b_n(T) \end{pmatrix} = F\begin{pmatrix} a_n(0) \\ b_n(0) \end{pmatrix}, \tag{22}$$

where F is the Floquet matrix. Linear stability of the solution $\Psi_n^{(0)}(t)$ requires that the matrix F has no eigenvalues of modulus larger than one; otherwise the solution will be linearly unstable. We have proved numerically that the Floquet eigenvalues stay on the unit circle ensuring linear stability for the stationary localized solutions derived from the homoclinic map orbit.

III. PERIODIC, QUASIPERIODIC, AND CHAOTIC LOCALIZED SOLUTIONS

A. The single oscillator

In this section we investigate the dynamical properties of a single damped, driven oscillator. For vanishing couplings $V=0$ results a lattice of uncoupled oscillators, each obeying the equation

$$i\dot{\Phi}+2|\Phi|^2\Phi = h\exp(i\Omega t)\Phi^* - i\delta\Phi. \tag{23}$$

In order to apply perturbational methods such as the averaging procedure we consider the case of weak driving force and small damping, i.e., h and δ are assumed to be small. For the forthcoming analysis it is useful to perform a phase transformation

$$\Phi(t)=\exp(i\omega t)\tilde{\Phi}(t), \tag{24}$$

yielding the modified oscillator equation

$$i\dot{\tilde{\Phi}}+2|\tilde{\Phi}|^2\tilde{\Phi}-\omega\tilde{\Phi} = h\exp(i\tilde{\Omega}t)\tilde{\Phi}^* - i\delta\tilde{\Phi}, \tag{25}$$

where we used $\tilde{\Omega}=\Omega-2\omega$. For ease of notation we drop the tildes again. Writing $\Phi=X+iY$ and decomposing into real and imaginary parts gives

$$\dot{X} = \omega Y - 2(X^2+Y^2)Y - h[\cos(\Omega t)Y-\sin(\Omega t)X]-\delta X, \tag{26}$$

$$\dot{Y} = -\omega X + 2(X^2+Y^2)X - h[\cos(\Omega t)X+\sin(\Omega t)Y]-\delta Y. \tag{27}$$

We are interested in periodic forced responses of the oscillator that can be expected when the system is close to a resonance of order k, i.e., when $\Omega\simeq k\omega$ for integer k. To cast the resonant system into the form appropriate for applying the averaging method [26] we use the invertible van der Pol transformation

$$\begin{pmatrix} u \\ v \end{pmatrix} = A\begin{pmatrix} X \\ Y \end{pmatrix}, \quad A=\begin{bmatrix} \cos(k^{-1}\Omega t) & -\sin(k^{-1}\Omega t) \\ -\sin(k^{-1}\Omega t) & -\cos(k^{-1}\Omega t) \end{bmatrix}, \tag{28}$$

under which the system (26) and (27) becomes

$$\dot{u} = (k^{-1}\Omega-\omega)v + 2(u^2+v^2)v - \delta u +h\{2\cos(k^{-1}\Omega t)\sin(k^{-1}\Omega t)[\cos(\Omega t)u-\sin(\Omega t)v] +[\cos^2(k^{-1}\Omega t)-\sin^2(k^{-1}\Omega t)][\sin(\Omega t)u +\cos(\Omega t)v]\}, \tag{29}$$

$$\dot{v} = -(k^{-1}\Omega-\omega)u - 2(u^2+v^2)u - \delta v -h\{2\cos(k^{-1}\Omega t)\sin(k^{-1}\Omega t)[\cos(\Omega t)v+\sin(\Omega t)u] -[\cos^2(k^{-1}\Omega t)-\sin^2(k^{-1}\Omega t)][\cos(\Omega t)u -\sin(\Omega t)v]\}, \tag{30}$$

with $|k^{-1}\Omega-\omega|\ll 1$. Since $\dot{u}$ and $\dot{v}$ are small the functions u and v vary slowly and we can approximate the right-hand sides of Eqs. (29) and (30) by averaging over one period $T=2\pi/\Omega$. The integration has to be performed individually for each value of k. Later $k=2$ is used, for which we obtain

$$\dot{u} = (2^{-1}\Omega-\omega)v + 2(u^2+v^2)v - \delta u + \frac{h}{5\pi}u, \tag{31}$$

$$\dot{v} = -(2^{-1}\Omega-\omega)v - 2(u^2+v^2)v - \delta u + \frac{h}{5\pi}v. \tag{32}$$

Expressing the averaged system in polar coordinates $u=r\cos\phi$ and $v=r\sin\phi$ gives

$$\dot{r}=[-\delta+\hat{h}\cos 2\phi]r, \tag{33}$$

$$\dot{\phi}=-(\hat{\Omega}+2r^2+\hat{h}\sin 2\phi), \tag{34}$$

where we used the notations $\hat{\Omega}=2^{-1}\Omega-\omega$ and $\hat{h}=h/5\pi$. The transformation (28) relates the original functions X,Y with u,v and r,ϕ, respectively, via

$$\begin{aligned} x(t)&=\cos(k^{-1}\Omega t)u(t)-\sin(k^{-1}\Omega t)v(t)\\ &=r(t)\cos[k^{-1}\Omega t+\phi(t)],\\ y(t)&=-[\sin(k^{-1}\Omega t)u(t)+\cos(k^{-1}\Omega t)v(t)]\\ &=-r(t)\sin[k^{-1}\Omega t+\phi(t)], \end{aligned}$$

showing that equilibria of the averaged system correspond to almost sinusoidal solutions of the original equations.

Nontrivial fixed points $\bar{r},\bar{\phi}$ are located at

$$\bar{r}=\sqrt{-\frac{1}{2}\left[\hat{\Omega}\pm\hat{h}\sqrt{1-\left(\frac{\delta}{\hat{h}}\right)^2}\right]}, \tag{35}$$

$$\bar{\phi}=\frac{1}{2}\cos^{-1}\left(\frac{\delta}{\hat{h}}\right). \tag{36}$$

We obtain the stability properties of the fixed points by considering the eigenvalues of the linearized averaged system, which are given by

$$\lambda=-\delta\pm\{-4\hat{h}^2+5\delta^2\mp 4\hat{\Omega}\sqrt{\hat{h}^2-\delta^2}\}^{-1/2}. \tag{37}$$

The analytical expression (37) is used for identifying parameter constellations for which the averaged system has stable fixed points ($\mathrm{Re}\,\lambda<0$), the locations of which are then determined by Eqs. (35) and (36). These stable equilibria of the averaged system provide then stable oscillatory modes of the original equations of the single oscillator. The results of the investigation of the single oscillator (regarded as uncoupled from the lattice for $V=0$) are the basis for the forthcoming studies of the DNLS lattice of weakly coupled, damped, and driven oscillators. In particular the situation for which only one lattice oscillator performs stable oscillatory motions whereas all the others are unexcited and the interoscillator coupling strength V is small complies with single-site excitation of the anti-integrable limit [25].

B. Stationary localized solutions and bifurcation to quasiperiodic breathers

In this section we describe the dynamics of the various types of localized states appearing for the damped, driven DNLS lattice. In our approach we start from the anticoupling limit arising for vanishing couplings $V=0$ and use one-site excitations for which all but one oscillator is at rest. This provides trivial spatially localized solutions. For small couplings we expect that this trivial localized single-site state persists as an exponentially localized lattice excitation. In [27] a similar approach has been used to excite breathers in a chain of nonlinear oscillators subject to periodic parametric driving. Therefore, we take parameters such that an uncoupled oscillator operates in the regime of bistability for which besides the stable zero solution a second nonzero stable oscillatory mode exists (see Sec. III A). In order to generate localized lattice states we excite only the central oscillator at $n=250$ initially while the rest of the lattice oscillators are held at rest (local stable zero solution). Concerning the initial conditions of the excited central oscillator, we remark that they do not necessarily have to coincide with the exact position of the attractor (the sink) on the Poincaré map of a single uncoupled oscillator. Rather the initial conditions can be taken at any location contained in the corresponding basin of attraction. In fact, after a transient the dynamics reaches a steady state. This relaxation onto an attractor makes the excitation of localized states in a damped (and driven) lattice system easier than in Hamiltonian lattices. In the latter case a numerical scheme based on the continuation from the no-coupling limit is used, requiring comparatively more effort for the computation of breathers [28] than for damped lattices, where it suffices to use initial conditions lying in the domain of the basis of attraction. We integrated numerically the lattice system consisting of 500 oscillators imposing periodic boundary conditions. Figure 3(a) depicts the excitation pattern for a coupling strength of $V=0.1$, where we omitted a transient of $T=500$. One clearly recognizes a coherent stable spatial structure in the form of a stationary state exponentially localized around the site $n=250$. A comparison of the localized steady amplitude pattern of Fig. 3 with the one of the corresponding solitonlike state gained from the homoclinic orbit of the stationary map analysis (see Sec. II) reveals their coincidence. Hence, after a transient period the initial single site excitation of the lattice

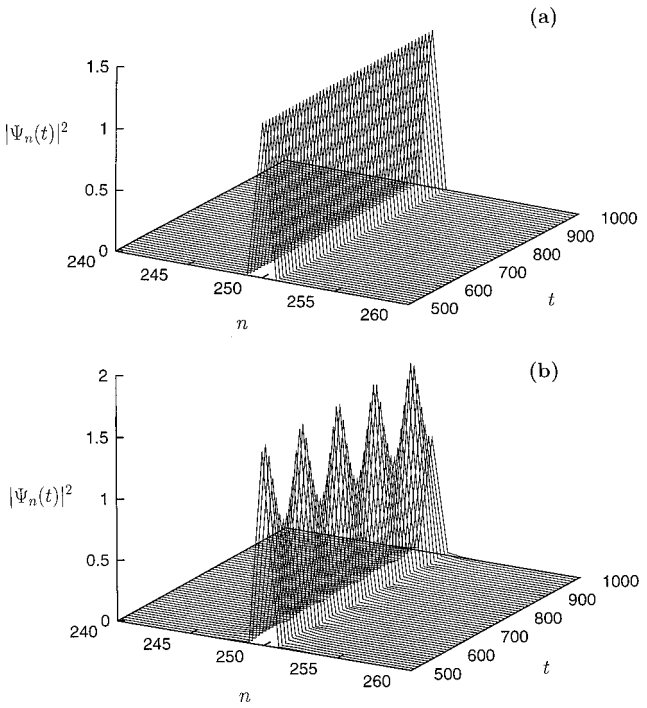

FIG. 3. Excitation pattern of the damped, driven lattice. (a) Steady localized amplitude profile. The parameters are $\delta=0.01$, $\omega=1$, $\Omega=2$, $V=0.1$, and $h=0.35$. (b) Breathing localized amplitude profile. The parameters are the same as in (a), except for the increased driving force amplitude $h=0.38$.

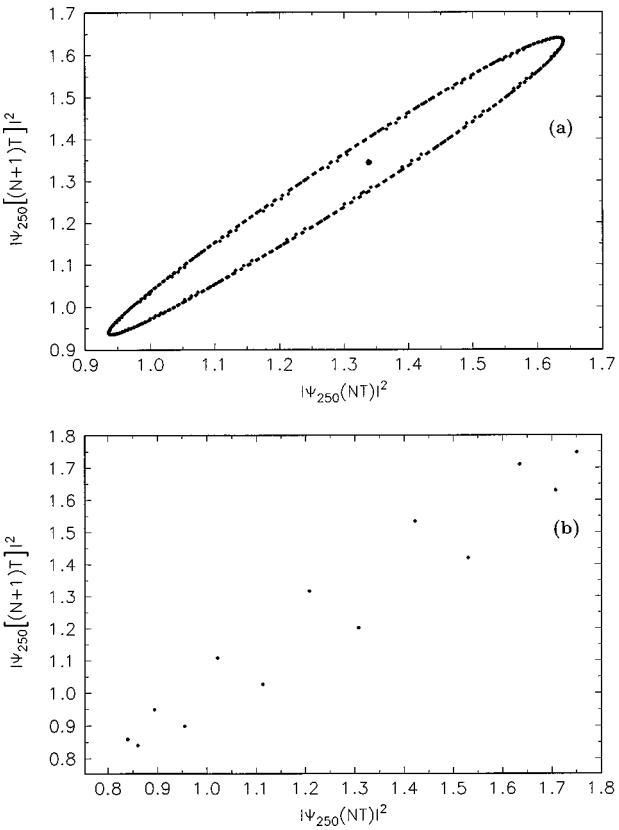

FIG. 4. First return map $|\Psi_{250}[(N+1)T]|^2-|\Psi_{250}(NT)|^2$ with period $T=2\pi/\Omega$. (a) The parameters are the same as in Fig. 3(a), yielding the fixed point at (1.34, 1.34), respectively, as in Fig. 3(b), giving the filled circular orbit around the fixed point. (b) The parameters are the same as in (a), except for the enlarged amplitude $h=0.393\,35$, resulting in a set of discrete points associated with periodic motion.

merges dynamically into a stationary solitonlike solution. The pattern of the latter involves besides the large amplitude of the central oscillator also the smaller amplitudes of the next two lattice oscillators on either side of it while the rest of the vanishingly small lattice amplitudes form the exponential tail of the localized state. In this sense the stationary solitonlike solution acts as a global attractor for the dynamics for a single-site excitation of the damped, driven DNLS lattice.

For further dynamical studies we keep the parameters ω, Ω, V, and δ fixed and vary the amplitude of the driving force. The steady solitonlike state persists up to a driving force strength of $h<0.38$. Increasing the amplitude of the driving force to $h=0.38$ causes temporal oscillations of the excitation pattern maintaining its localized structure. Figure 3(b) shows the breathing localized amplitude pattern.

Due to the spatial coherence the lattice dynamics can be characterized by a local picture of a single oscillator taken to be the central one at lattice site $n=250$. A reduction of the lattice dynamics is achieved by the two-dimensional return map. To this end the time series of the central site amplitude is observed stroboscopically at the period of the driving force. We obtain then a set of discrete data $|\Psi_{250}(NT)|^2$, $N=1,2,\ldots,$ and $|\Psi_{250}((N+1)T)|^2$ is plotted as a function of $|\Psi_{250}(NT)|^2$ in Fig. 4.

In the case of the stationary localized state shown in Fig. 3(a) for which the amplitudes $|\Psi_{250}(NT)|^2$ remain constant (likewise, the amplitudes of all the other oscillators apart from $n=250$) the return map shows only one fixed point. In the case of the breathing localized pattern of Fig. 3(b) the $|\Psi_{250}((N+1)T)|^2-|\Psi_{250}(NT)|^2$ plot yields a closed circular orbit around the fixed point. Since the trajectory densely covers the circular loop, quasiperiodic motion is indicated. In fact, the corresponding power spectrum of the time evolution of the central amplitude shows the presence of two incommensurate frequencies confirming the quasiperiodicity of the dynamics (not shown for this case but see also further below).

We conclude that at a driving amplitude $h=0.38$ a Hopf bifurcation takes place. As a result, the trajectory of the return map of each lattice oscillator changes from a fixed point to motion on a limit cycle. The dynamical amplitude profile of the lattice oscillators performs then a transition from a stationary localized state to a *quasiperiodic breather*.

Qualitatively equal pictures can be obtained for the local return maps of all the other oscillators. However, we can deduce from the local properties of a single two-dimensional return map the global properties of the lattice of coupled oscillators with the use of phase correlation functions. We pass to polar coordinates $\Psi_n=r_n\exp(i\theta_n)$ and define a phase correlation function at a fixed instant of time as

$$C(m)=\langle\theta_{m+1}\theta_m\rangle=\frac{1}{N-m}\sum_{n=1}^{N-m}\theta_n\theta_{n+m},\quad 1\leqslant m\leqslant N-1, \tag{38}$$

which enables us to distinguish between periodic and quasiperiodic lattice states. For mutually periodically oscillating lattice oscillators their phases are correlated and all correlation functions $C(m)$ remain constant, while for quasiperiodic breathers due to the loss of phase coherences the correlation functions decay.

For $h=0.393\,35$ the breathing of the amplitudes is periodic, as is indicated by the set of discrete points on the corresponding return map of Fig. 4(b). The excitation pattern of the frequency locked lattice oscillations is governed by a *periodic breather*.

C. Torus destruction, spatiotemporal chaos, and collapse to localized multisite states

When the driving force amplitude is further increased we observe a dynamical bifurcation, that is, the character of motion changes in the course of time. For an appropriate illustration of the rich dynamical features we plot in Fig. 5 the time evolution of the central site amplitude. A first time interval is characterized by regular (quasiperiodic) motion followed by a chaotic transient, which finally ends up in a steady state of constant amplitude. Concerning the dynamics of the lattice excitation, we depict in Fig. 6 the amplitude profiles of the lattice for three time intervals belonging to the qualitatively different scenarios of Fig. 5. We note that in an initial time interval the localized excitation pattern persists as a quasiperiodic breather on the lattice corresponding to stable torus motion [Fig. 6(a)]. However, at $t\cong 2000$ this torus is destroyed and the motion becomes unstable. As a

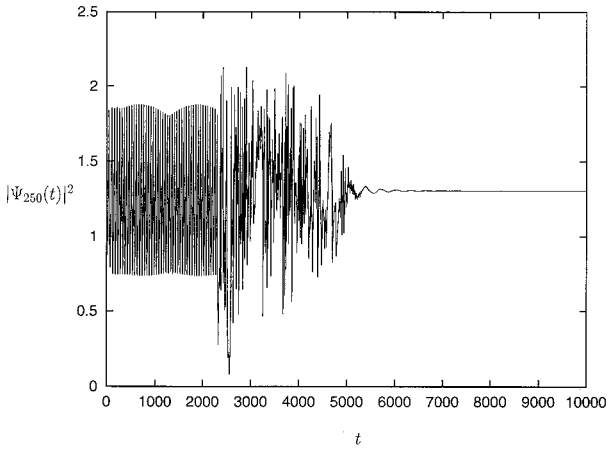

FIG. 5. Time evolution of the amplitude of the central oscillator. The parameters are the same as in Fig. 3, except for the increased amplitude $h=0.408$.

consequence, the lattice dynamics exhibits spatiotemporal chaos. Remarkably, the chaotic dynamics is spatially confined to a few (<10) lattice sites, whereas the rest of the lattice remains unexcited [Fig. 6(b)]. Thus we call this localized structure a *chaotic breather*. The transition from a quasiperiodic lattice motion to chaotic dynamics is reflected in the power spectra attributed to the trajectory of the central oscillator. Figures 7(a) and 7(b) display the power spectra of $|\Psi_{250}(t)|^2$ for the time intervals $500 \leqslant t \leqslant 1524$ and $2500 \leqslant t \leqslant 3024$, respectively. The former power spectrum shows peaks at incommensurate frequencies typical of quasiperiodic motion, while for the last one we note the broadband character associated with chaotic time evolution. Finally, at $t \approx 5500$ the chaotic interlude stops and the dynamics relaxes to a lasting steady state [Fig. 6(c)]. Contrary to the exponential localization around a single site in the beginning, the final localized steady amplitude profile of the lattice involves now six sites of almost equal amplitudes. Linear stability of the final multisite stationary localized state is proved with the help of Floquet analysis (see Sec. II). Note that the quasiperiodic phase and the duration of the chaotic breather are fairly long, meaning that both exist for more than 600 periods of the driving force.

Finally, above a driving amplitude of $h=0.409$ the lattice dynamics runs initially through a regime of localized spatiotemporal chaos. For $t \geqslant 2500$ the excitation pattern eventually decays to a stable state of vanishing amplitudes, i.e., all lattice oscillators approach their local zero attractor, as illustrated in Fig. 8 for $h=0.4095$.

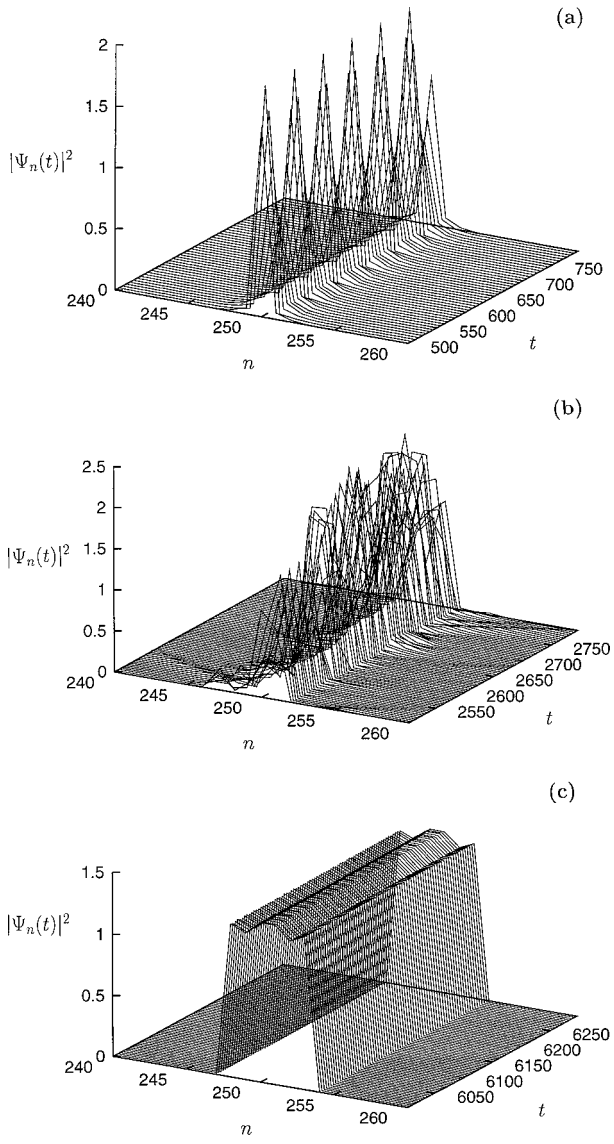

FIG. 6. Excitation pattern of the damped, driven lattice for different time intervals showing the dynamical bifurcations from a quasiperiodic breather via a chaotic breather to a stable steady multisite localized state. (a) The quasiperiodic breather. (b) The chaotic breather. (c) The steady multisite localized state.

IV. SUMMARY AND CONCLUSIONS

We studied the dynamical properties of a damped, parametrically driven DNLS with focus on the existence and stability of localized solution. In the first part of the paper we established the existence and stability of a static solitonlike lattice state of the damped and parametrically driven DNLS lattice. Such a stationary localized state exists if the energy loss due to dissipation is balanced by a proper energy injection through the driving force. In order to construct the localized solution we exploited a nonlinear map approach. We identified parameter ranges for which the origin of the four-dimensional map represents a hyperbolic equilibrium. Its associated homoclinic orbit supports a stationary solitonlike solution on the lattice, the linear stability of which is proved by a Floquet analysis.

The second part of the paper was devoted to the dynamical properties of localized lattice excitations. We demonstrated that, dependent upon the amplitude of the driving force, static bifurcations take place so that the character of the localized lattice states changes from static to time-oscillating solutions. These oscillations can be of either periodic or quasiperiodic nature. Furthermore, we detected dynamical bifurcations for which regular quasiperiodic motion is destabilized in the course of time and a transient of spatiotemporal chaos appears, forming a localized chaotically breathing lattice state. After this chaotic interlude follows a relaxation of the lattice oscillators to a stable localized multisite amplitude pattern.

The temporal destabilization of the quasiperiodic motion

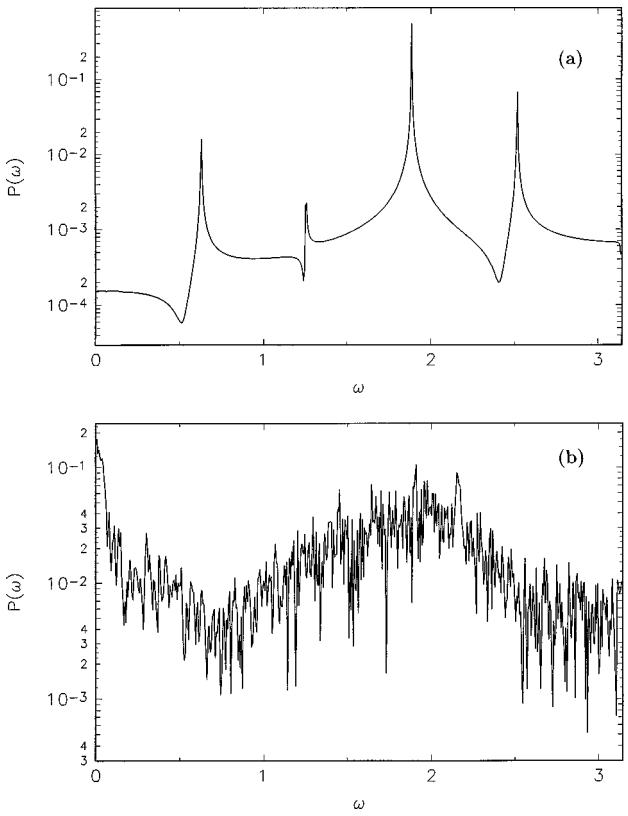

FIG. 7. Power spectrum of the amplitude $|\Psi_{250}(t)|^2$ of Fig. 5 for (a) $500 \leqslant t \leqslant 1524$ belonging to the regular quasiperiodic regime shown in Fig. 5 and (b) $2500 \leqslant t \leqslant 3024$ when the trajectory is chaotic.

accompanied by the destruction of the corresponding torus in phase space reported in this paper has to be compared with previous results on torus destruction. In [29] a cascade of torus doubling was identified as the destabilization mechanism of localized structures in continuous media modeled by a quintic complex Ginzburg-Landau equation. In directly driven sine-Gordon and NLS equations the scenarios of period doublings and the quasiperiodic route to chaos were observed [30–34]. All these static bifurcation scenarios stem from the variation of a parameter of the underlying equations. Additionally, in our case a dynamical bifurcation also occurs for which destabilization appears after a transient period of regular evolution at fixed parameters.

At this stage it is suitable to compare directly our results of the investigation of the damped, driven DNLS equation with those for its continuum counterpart, namely, the damped, driven NLS equation explored in [2,8]. To mention the properties that the continuum and the lattice equation

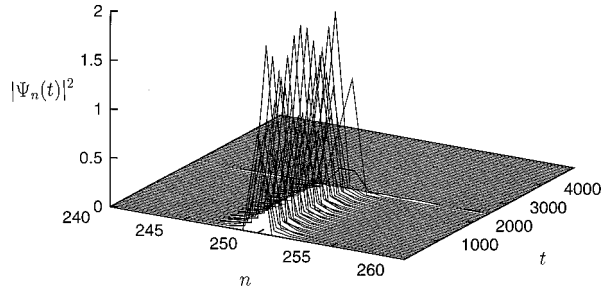

FIG. 8. Amplitude profile of the damped, driven lattice demonstrating the decay of a chaotic breather to zero lattice amplitudes. The parameters are the same as in Fig. 3, except for $h = 0.4095$.

share we note that for both of them stationary soliton solutions have been found. Furthermore, when increasing the driver amplitude these stationary solitons undergo bifurcations to periodic and quasiperiodic breatherlike localized excitations. Finally, above a certain driver amplitude the breathing solitons become unstable and spatiotemporal chaos sets in. For the NLS equation the transition to chaos occurs via the route of a period doubling or a quasiperiodic scenario [8]. In the case of the DNLS we did not observe such a transition to chaos. As mentioned earlier, the order-chaos transition is the outcome of a dynamical destabilization process for which quasiperiodic motion develops into chaos in the course of time. Thus we call this transition a *dynamical quasiperiodic route*. Contrary to the strong spatial confinement of the chaos in our present study of the damped, driven DNLS lattice, the chaos in the case of the NLS equation is extended all over the spatial dimension of the one-dimensional structure. Apparently, the localization of chaos for the DNLS equation is a pinning effect due to the lattice discreteness supporting a low-dimensional attractor for a spatially extended system. As far as the DNLS equation is concerned, the chaotic breather serves as the source for the creation of a localized multisite state. This temporal transition from an initial coherent structure (the single-pulse soliton) via an interlude of chaos to a final stable coherent structure of spatially extended excitation peak is a different effect. Finally, above a critical amplitude of the parametric driving force the solitonlike excitation fades away and leaves the lattice oscillators at their stable zero rest positions (zero attractor). This happens for both the continuum NLS equation [8] and its discrete DNLS counterpart.

ACKNOWLEDGMENT

This work was supported by the Deutsche Forschungsgemeinschaft via Sonderforschungsbereich 337.

[1] V. E. Zakharov, V. S. L'vov, and S. S. Starobinets, Sov. Phys. Usp. **17**, 896 (1975).

[2] I. V. Barashenkov, M. M. Bogdan, and V. I. Korobov, Europhys. Lett. **15**, 113 (1984).

[3] J. Wu, R. Keolian, and I. Rudnick, Phys. Rev. Lett. **52**, 1421 (1984).

[4] H. Yamazaki and M. Mino, Prog. Theor. Phys. Suppl. **98**, 400 (1989).

[5] V. E. Zakharov, S. L. Musher, and A. M. Rubenchik, Phys. Rep. **129**, 285 (1985).

[6] L. D. Faddeev and L. A. Takhtajan, *Hamiltonian Methods in the Theory of Solitons* (Springer-Verlag, Berlin, 1987).

[7] J. W. Miles, J. Fluid Mech. **148**, 451 (1984).
[8] M. Bondila, I. V. Barashenkov, and M. M. Bogdan, Physica D **87**, 314 (1995).
[9] T. Holstein, Ann. Phys. (N.Y.) **8**, 325 (1959); J. C. Eilbeck, P. S. Lomdahl, and A. C. Scott, Physica D **16**, 318 (1985); V. M. Kenkre and D. K. Campbell, Phys. Rev. B **34**, 4955 (1986); A. S. Davydov and N. I. Kislukha, Phys. Status Solidi B **59**, 465 (1973); D. N. Christodoulides and R. I. Joseph, Opt. Lett. **13**, 794 (1988); N. Finlayson and G. I. Stegeman, Appl. Phys. Lett. **56**, 2276 (1990); Y. Chen, A. W. Snyder, and D. J. Mitchell, Electron. Lett. **26**, 77 (1990); M. I. Molina, W. D. Deering, and G. P. Tsironis, Physica D **66**, 135 (1993); H. Feddersen, P. L. Christiansen, and M. Salerno, Phys. Scr. **43**, 353 (1991); L. J. Bernstein, Opt. Commun. **94**, 406 (1992); D. Hennig, Physica D **64**, 121 (1993); Yu. S. Kivshar, Phys. Rev. E **48**, 4132 (1993); A. B. Aceves, C. De Angelis, T. Peschel, R. Muschall, F. Lederer, S. Trillo, and S. Wabnitz, *ibid.* **53**, 1172 (1996); D. Hennig and G. P. Tsironis, Phys. Rep. **307**, 333 (1999).
[10] R. Scharf and A. R. Bishop, Phys. Rev. A **43**, 6535 (1991).
[11] B. M. Herbst and M. J. Ablowitz, Phys. Rev. Lett. **62**, 2065 (1989).
[12] D. Hennig, K. Ø. Rasmussen, H. Gabriel, and A. Bülow, Phys. Rev. E **54**, 5788 (1996).
[13] R. S. MacKay and S. Aubry, Nonlinearity **7**, 1623 (1994).
[14] S. Flach and C. R. Willis, Phys. Rep. **295**, 181 (1998).
[15] J. A. Sepulchere and R. S. MacKay, Nonlinearity **10**, 679 (1997).
[16] M. Johansson and S. Aubry, Nonlinearity **10**, 1151 (1997).
[17] D. Cai, A. R. Bishop, and N. Grønbech Jensen, Phys. Rev. E **52**, 5784 (1995).
[18] M. J. Ablowitz and P. A. Clarkson, *Solitons, Nonlinear Evolution Equations and Inverse Scattering* (Cambridge University Press, New York, 1991).
[19] M. J. Ablowitz and J. F. Ladik, J. Math. Phys. **17**, 1011 (1976).
[20] V. V. Konotop, O. A. Chubykalo, and L. Vázquez, Phys. Rev. E **48**, 563 (1993).
[21] D. Cai, A. R. Bishop, and N. Grønbech Jensen, Phys. Rev. E **53**, 4131 (1996).
[22] P. L. Christiansen, Yu. B. Gaididei, M. Johansson, and K. Ø. Rasmussen, Phys. Rev. B **55**, 5759 (1997).
[23] J. E. Howard and R. S. MacKay, J. Math. Phys. **28**, 1036 (1987).
[24] A. J. Lichtenberg and M. A. Liebermann, *Regular and Stochastic Motion* (Springer-Verlag, New York, 1988).
[25] S. Aubry, Physica D **103**, 1 (1997).
[26] A. H. Nayfeh and D. T. Moon, *Nonlinear Oscillations* (Wiley, New York, 1979).
[27] M. Abel and A. Pikovsky, Z. Naturforsch., A: Phys. Sci. **52**, 570 (1997).
[28] J. L. Marin and S. Aubry, Nonlinearity **9**, 1501 (1996).
[29] J. I. Kim, H. K. Park, and H. T. Moon, Phys. Rev. E **55**, 3948 (1997).
[30] K. Nozaki and N. Bekki, Physica D **21**, 381 (1986).
[31] K. H. Spatschek, H. Pietsch, E. W. Laedke, and Th. Eickermann, in *Singular Behavior and Nonlinear Dynamics*, edited by T. Bountis and St. Pnevmatikos (World Scientific, Singapore, 1989).
[32] A. R. Bishop, M. G. Forest, D. W. McLaughlin, and E. A. Overman, Physica D **23**, 293 (1986).
[33] M. Taki, K. H. Spatschek, J. C. Fernandez, R. Grauer, and G. Reinisch, Physica D **40**, 65 (1989).
[34] G. Terrones, D. W. McLaughlin, and A. J. Pearlstein, SIAM (Soc. Ind. Appl. Math.) J. Appl. Math. **50**, 791 (1990).